Gazi Üniversitesi
Fen Bilimleri Dergisi
PART C: TASARIM VE TEKNOLOJİ

Gazi University
Journal of Science
PART C: DESIGN AND TECHNOLOGY

GU J Sci, Part C, 12(2): 719-728 (2024)

Efficiency Optimization of Multiple Coil Wireless Power Transfer System based on Adaptive Impedance Matching Network

Fatih ISSI[1*]

[1]*Cankiri Karatekin University, Vocational High School, Electronics and Automation Department, Cankiri, Turkey*

Article Info

Research article
Received: 31/03/2024
Revision: 29/04/2024
Accepted: 09/05/2024

Keywords

Multi-Coil Transmitter
Wireless Power Transfer
Wireless Power
Transmission Efficiency

Makale Bilgisi

Araştırma makalesi
Başvuru: 31/03/2024
Düzeltme: 29/04/2024
Kabul: 09/05/2024

Anahtar Kelimeler

Çok Bobinli Verici
Kablosuz Güç Aktarımı
Kablosuz Güç Aktarım
Verimi

Graphical/Tabular Abstract (Grafik Özet)

A study on wireless energy transfer using a system with multiple coils and a full bridge inverter at 85 kHz showed efficiency improvements with an adaptive capacity array, achieving 87.5-91.9% efficiency. Efficiency increased in five locations and decreased in three others after impedance matching. / Birden fazla verici bobine sahip, 85 kHz'de tam köprü invertör kullanılarak hazırlanan bir kablosuz enerji aktarımı sistemi için, adaptif kapasite dizisi kullanılarak %87,5-91,9 aralığında verim elde edilen bir verimlilik iyileştirme çalışması sunulmuştur. Çalışmada, kapasite ayarlamasından sonra verim, alıcı bobinin yerleştirildiği beş konumda artmış ve diğer üç konumda ise azalmıştır.

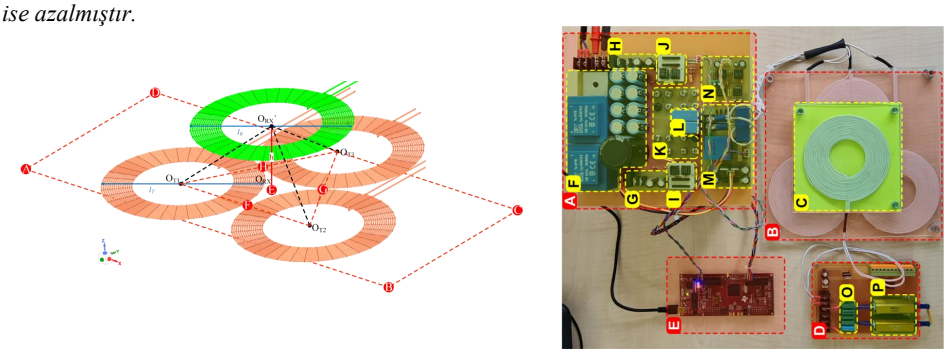

Figure A: *Ansys Maxwell receiver coil layout with transmitter coils and main parts of the experimental set / **Şekil A:** Ansys Maxwell alıcı bobin ve verici bobinlere ait yerleşim düzeni ve deney setinin ana bileşenleri.*

Highlights (Önemli noktalar)

- *An innovative wireless power transfer system employing multiple transmitter coils / Birden fazla verici bobini kullanan yenilikçi bir kablosuz güç aktarım sistemi*
- *Simulation and experimental study for wireless power transmission efficiency change analysis/ Kablosuz güç aktarım verim değişim analizi için benzetim ve deneysel çalışma*
- *Importance of receiver coil placement in wireless power transfer systems / Kablosuz güç aktarım sistemlerinde alıcı bobin yerleşiminin önemi*

Aim (Amaç): *The aim of the document is to assess the impact of a adaptive capacity array on the efficiency of a wireless energy transfer system for various receiver coil placements. / Çalışmanın amacı, çeşitli alıcı bobin konumları için adaptif kapasite dizisinin kablosuz enerji aktarım sisteminin verimliliği üzerindeki etkisini değerlendirmektir.*

Originality (Özgünlük): *Adaptive impedance matching for a multi-coil wireless energy transfer system using adaptive capacity array is the unique aspect of this study / Adaptif kapasite dizisi kullanılarak çoklu bobinli kablosuz enerji aktarım sistemi için adaptif empedans uyumlamasının yapılması bu çalışmanın özgün tarafıdır.*

Results (Bulgular): *The simulation and experimental study both showed efficiency ranging from 87.5% to 91.5%. The tuned capacity array was used in both studies, resulting in efficiency ranging between 89.3% and 92.8% in the simulation and between 89.5% and 93.1% in the experimental study. / Benzetim ve deneysel çalışmalarının her ikisi de %87,5 ile %91,5 arasında değişen verimlilik göstermiştir. Her iki çalışmada da adaptif kapasite dizisi kullanılmış, bu da simülasyonda %89,3 ile %92,8 arasında ve deneysel çalışmada %89,5 ile %93,1 arasında değişen verimlilikle sonuçlanmıştır.*

Conclusion (Sonuç): *In cases where the adaptive capacity array was used, the efficiency increased in some coil positions and decreased in others. It was concluded that the resolution of the capacity array should be increased. / Adaptif kapasite dizisinin kullanıldığı durumlarda bazı bobin konumlarında verim artmış, bazı konumlarda ise verim azalmıştır. Kapasite dizisinin çözünürlüğünün artırılması gerektiği sonucuna varılmıştır.*

*Corresponding author, e-mail: fatihissi@karatekin.edu.tr
DOI: 10.29109/gujsc.1462208

GU J Sci, Part C, 12(2): 719-728 (2024)

Gazi Üniversitesi
Fen Bilimleri Dergisi
PART C: TASARIM VE TEKNOLOJİ

Gazi University
Journal of Science
PART C: DESIGN AND TECHNOLOGY

http://dergipark.gov.tr/gujsc

Efficiency Optimization of Multiple Coil Wireless Power Transfer System based on Adaptive Impedance Matching Network

Fatih ISSI[1*]

[1]*Cankiri Karatekin University, Vocational High School, Electronics and Automation Department, Cankiri, Turkey*

Article Info

Research article
Received: 31/03/2024
Revision: 29/04/2024
Accepted: 09/05/2024

Keywords

Multi-Coil Transmitter
Wireless Power Transfer
Wireless Power Transmission Efficiency

Abstract

A wireless energy transfer system was developed using multiple transmitting coils and a full bridge inverter at 85 kHz. The system consisted of three identical transmitter coils and one receiver coil. The study aimed to assess the impact of a tuned capacity array on the system's efficiency for various receiver coil placements. The experiment was conducted in eight different placements, with and without capacity tuning. The simulation showed that the efficiency ranged from 87.5% to 91.5%, while the experimental study showed efficiency between 87.8% and 91.9% under the same conditions. The tuned capacity array was utilized in both studies, resulting in efficiency ranging between 89.3% and 92.8% in the simulation and between 89.5% and 93.1% in the experimental study. The experiment revealed an increase in efficiency of 1.65%, 1.23%, 1.39%, 2.5%, and 1.28% in five different locations (A→E), respectively, while a decrease of 0.4%, 0.89%, and 0.45% was observed in three other locations (F→H), respectively.

Adaptif Empedans Eşleştirme Ağı Tabanlı Çok Bobinli Kablosuz Güç Aktarım Sisteminin Verimlilik Optimizasyonu

Makale Bilgisi

Araştırma makalesi
Başvuru: 31/03/2024
Düzeltme: 29/04/2024
Kabul: 09/05/2024

Anahtar Kelimeler

Çok Bobinli Verici
Kablosuz Güç Aktarımı
Kablosuz Güç Aktarım Verimi

Öz

Çoklu verici bobine sahip, 85 kHz anahtarlama frekansında çalışan tam köprü invertör kullanılarak bir kablosuz enerji transfer sistemi geliştirilmiştir. Sistem, üç özdeş verici bobin ve bir alıcı bobinden oluşmaktadır. Çalışmada, adaptif kapasite dizisi kullanılarak, farklı alıcı bobin konumlarında sistemin verim değişimi analiz edilmiştir. Kapasite dizinin ayarlandığı ve ayarlanmadığı sekiz farklı bobin yerleşimi için benzetim ve deneysel çalışmalar yapılmıştır. Ayarlı kapasite dizisinin uygulanmadığı benzetim çalışması, verimin %87,5 ile %91,5 arasında değiştiğini gösterirken, deneysel çalışma aynı koşullar altında %87,8 ile %91,9 arasında değiştiğini göstermiştir. Ayarlı kapasite dizisinin uygulandığı durumda ise, benzetim çalışması için %89,3 ile %92,8 aralığında, deneysel çalışmada ise %89,5 ile %93,1 arasında değişen verim değerleri elde edilmiştir. Adaptif kapasite dizisi uygulandığında elde edilen deneysel çalışma sonuçları, beş farklı konumda (A→E) sırasıyla %1.65, %1.23, %1.39, %2.5 ve %1.28'lik bir verimlilik artışı ortaya koyarken, diğer üç konumda (F→H) sırasıyla %0.4, %0.89 ve %0.45'lik bir düşüş meydana geldiğini göstermiştir.

1. INTRODUCTION (GİRİŞ)

In typical two-coil wireless power transmission (WPT) systems, the maximum output power can be achieved at an optimal transmission distance that satisfies the critical connection condition between the transmitter (Tx) and receiver (Rx) coils [1]. However, the output power is significantly reduced outside the optimal transmission distance. Generally, wireless EV chargers can provide maximum load power in a center-aligned state, as this condition has maximum magnetic coupling[2-5]. Typical two-coil WPT systems are very responsive to the operating environment[6]. In an over-connected situation where the distance between the coils is shorter than the optimal transfer distance, the system inevitably acquires unnecessary reactance components, which decreases the output power at the operating frequency [7]. However, the magnetic coupling between the transmitter (Tx) coil and the receiver (Rx) coil rapidly decreases due to misalignment between the Tx and Rx coils, resulting in a reduced power distribution capacity; therefore, conventional Tx and Rx coil sets often have tight misalignment tolerances. Simple two-coil groups are not preferred due to the very low misalignment tolerance and the significant reduction of the magnetic coupling due

*Corresponding author, e-mail: fatihissi@karatekin.edu.tr
DOI: 10.29109/gujsc.1462208

to misalignment. Increasing the size of Tx and Rx coils based on the loop shape is just one of the methods to increase the tolerance for misalignment, but it is not practical due to the limitation of mounting areas for the coil set in vehicles[8]. The two most prominent misalignment problems observed in WPT systems are angular [9] and lateral[10] alignment. When studies are examined, automatically controlled alignment systems for central alignment can be used in EVs to guide EVs to charging stations, such as giant magnetoresistance (GMR) sensors or mobile communications [11, 12]. However, these guided systems require additional complex systems, and if the alignment systems fail, there may be a power distribution failure. To increase the tolerance for large misalignment, special coil structures can be used, for example, double D (DD), double D quadruple (DDQ), and bipolar (BP) pad [3-5, 13-15]. Although such coil structures can increase lateral misalignment tolerance, diagonal displacement becomes a significant issue as a potential worst-case scenario, as longitudinal and lateral displacements often occur simultaneously. Many studies focus on [16-21] to deal with misalignment problems. Although appropriate topologies are selected for specific operating conditions, reduced capacity to provide load power cannot be avoided if misalignments occur [16, 17]. Although the load power can be regulated under misalignment by various control methods such as frequency modulation control via in-band or out-band communication[18, 19], variable switching capacitance [20, 21], the power efficiency inevitably decreases, which eventually reduces system efficiency and results in heat dissipation of the Tx coils.

This study investigates the effect of mutual inductance analysis and power transmission efficiency analysis on the solution of the alignment problem in cases where variable switching capacitance is applied and not applied for a wireless energy transfer system with a multi-coil simple transmitter (Tx) structure. The simple structure of the coil structure is investigated to determine whether the efficiency can be increased without any structural changes in existing systems. Keeping the cost of transformation to a minimum in existing systems is the main focus of the study. In the study, circuit analysis for a wireless energy transfer system with three transmitting coils was carried out in Section 2, the analysis of impedance in alignment problems by finite element method was carried out in Section 3, and the change analysis of transmission efficiency with variable switched capacitance application was carried out in Section 4.

2. ANALYSIS (ANALİZ)

A wireless energy transfer system model with a simple coil structure involving three transmitter coils and one receiver coil has been studied. All three transmitter coils are identical to each other. The system has a high-frequency full-bridge inverter as a power source. The transmitter coils in the system are connected in series. The equivalent circuit of the system is given in Figure 1.

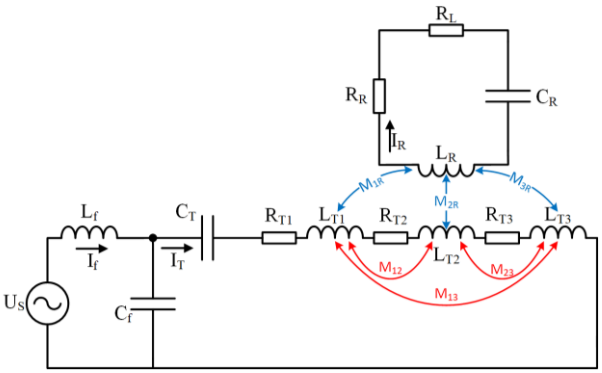

Figure 1. Equivalent circuit model of the wireless energy transfer system (Kablosuz enerji transfer sisteminin eşdeğer devre modeli)

L_f denotes the input impedance in the equivalent circuit, while C_f represents the capacitance in parallel. The transmitter coils are identified as L_{T1}, L_{T2}, and L_{T3} in the same circuit. The internal resistances of each transmitter coil are shown with R_{T1}, R_{T2}, and R_{T3}, respectively. C_T capacity is given to meet the resonance condition of the transmitting circuit. The input impedance of the transmitter circuit Z_f consists of the sum of the input inductance and parallel capacitance, which is given in Equation 1.

$$Z_f = j\omega L_f + \frac{1}{j\omega C_f} \qquad 1$$

The total inductance of the transmitter coils is expressed by L_{Tsum} given in Equation 2. In addition to containing the self-inductance L_{Ti} of each coil in the total inductance; it also contains the mutual inductance between the coils, which is one of the most important parameters for wireless energy transfer. Here, the fact that the transmitter coils are in a fixed position remains constant by not changing the mutual inductance between the coils.

$$L_{T_{sum}} = \sum_{i=1}^{3} L_{T_i} + 2\sum_{i=1}^{2}\sum_{h=i+1}^{3} M_{T_h T_i} \qquad 2$$

The equation expresses the mutual inductance as M_{ThTi} between the *h* and *i*'th coils. It constitutes the sum of the mutual inductance values M_{12} between the first and second coils, M_{23} between the second and third coils, and M_{13} between the first and third coils, respectively. The sum of the internal resistances of the transmitter coils are expressed in R_{Tsum} and is calculated as given in Equation 3:

$$R_{T_{sum}} = \sum_{i=1}^{3} R_{T_i} \qquad 3$$

After the parameters in the equivalent circuit are calculated in this way, the equivalent impedance of the transmitter circuit is calculated as follows.

$$Z_T = \frac{1}{j\omega C_f} + \frac{1}{j\omega C_T} + j\omega L_{T_{sum}} + R_{T_{sum}} \qquad 4$$

The transmitter circuit's equivalent impedance will be variable to create resonance conditions, regardless of whether the C_T capacity is constant or variable. In addition to the mutual inductance between transmitter coils, there is also mutual inductance between each transmitter and receiver coil. The mutual inductance between each *i*'th coil and the receiving coil is expressed as M_{TiR} and is calculated as presented in Equation 5.

$$M_{T_iR} = \sum_{i=1}^{3} M_{T_iR} + Z_{M_{T_iR}} \qquad 5$$

The equivalent impedance of the receiving circuit is expressed as Z_R as given in Equation 6. It consists of the sum of the self-inductance L_R of the receiving coil, the internal resistance R_R of the coil, the resonant capacity C_R and the receiver circuit load resistance R_L.

$$Z_R = j\omega L_R + \frac{1}{j\omega C_R} + R_R + R_L \qquad 6$$

For the transmitter circuit to achieve the resonance requirement in the system, the sum of the serial capacity C_T, the sum of the self-inductances of the coils L_{Ti} and their mutual inductances $M_{ThTi,}$ and the input inductance L_f must be equal to zero as given in Equation 7.

$$\frac{1}{j\omega C_T} + j\omega\left(\sum_{i=1}^{3} L_{T_i} + 2\sum_{i=1}^{3}\sum_{h=i+1}^{i-1} M_{T_hT_i} - L_f\right) = 0 \qquad 7$$

In this case, the source current I_T is equal to the ratio of the applied voltage *Us* to the input impedance $j\omega L_f$.

$$I_T = \frac{U_s}{j\omega L_f} \qquad 8$$

The I_R current passing through the receiving circuit varies depending on the transmitting circuit current. The I_T current flowing through the transmitting circuit induces a voltage in the receiving circuit depending on mutual inductance. The induced voltage passes the I_R current through the total resistance resistances of the receiving circuit $(R_R + R_L)$. When the I_T current obtained in Equation 8 is written in place as in Equation 9, a current relationship is established between the transmitter circuit and the receiving circuit.

$$I_R = \frac{j\omega M_{T_iR} I_T}{(R_R + R_L)} = \frac{U_s M_{T_iR}}{L_f(R_R + R_L)} \qquad 9$$

Receiving circuit power P_R is obtained as shown in Equation 10, depending on the current $I_T = U_s/j\omega L_f$ flowing through the transmitting circuit.

$$P_R = {I_R}^2 R_L = \frac{{U_s}^2\left(\sum_{i-1}^{3} M_{T_iR}\right)^2 R_L}{{L_f}^2(R_R + R_L)^2} \qquad 10$$

The total efficiency of the system η is given in Equation 11 by the ratio of the power transferred to the receiving circuit and the transmitter circuit power η.

$$\eta = \frac{|I_R|^2 R_L}{|I_T|^2 \sum_{i=1}^{3} R_{T_i} + |I_R|^2 (R_R + R_L)} = \frac{\frac{\omega^2\left(\sum_{i=1}^{3} M_{T_iR}\right)^2}{(R_R+R_L)^2} R_L}{\sum_{i=1}^{3} R_{T_i} + \frac{\omega^2\left(\sum_{i=1}^{3} M_{T_iR}\right)^2}{(R_R+R_L)}} \qquad 11$$

In this way, the efficiency η can be determined depending on the transmitter circuit power obtained due to the mutual inductance of each transmitter coil of the receiving circuit with the receiving coil M_{TiR} and the transmitter circuit power depending on the M_{TiR}. The efficiency analysis emphasized in Equation 4 is facilitated by the mutual inductance between the transmitter and receiver circuit. This allows for the variation analysis of M_{TiR} concerning the transmitter circuit's resonance capacity.

3. SIMULATION (BENZETİM)

Each self-inductance and mutual inductance value between the transmitter coils and the receiver coil was analyzed using the finite element method in Ansys Maxwell software. The analyzed coil layout

plan is given in Figure 2. In the analysis, the transmitter coil positions were fixed, and the receiver coil position was performed for eight positions from A to H points. The outer diameter of the coils used in the analysis is expressed as l_T, the outer diameter of the receiver coil is l_R, the height between the plane of the transmitter coil and the receiver coil h, and the distances between each transmitter coil and the other transmitter coil are expressed as D_{12}, D_{23}, D_{13}, respectively.

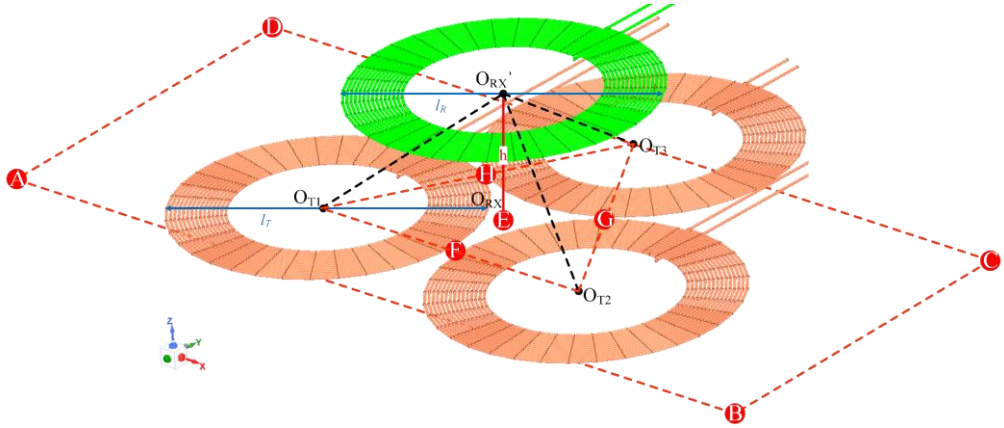

Figure 2. Ansys Maxwell receiver coil layout with transmitter coils (Verici bobinler ve Alıcı bobine ait Ansys Maxwell görünümü)

The center points of the transmitter coils are expressed as O_{T1}, O_{T2}, and O_{T3}, respectively, and the center point of the receiver coil is expressed as O_{RX}. All the mentioned parameters are given in Table 1.

Table 1. Distances between coils, layout positions, and distances between A→H points (Bobinler arasındaki uzaklıklar, bobin konumları ve A→H konumları arasındaki uzaklıklar)

	Distance (mm)						Position (x, y, z) (mm)			
Parameter.	**l_T**	**l_R**	**h**	**D_{12}**	**D_{13}**	**D_{23}**	**O_{T1}**	**O_{T2}**	**O_{T3}**	**O_{RX}'**
Value	250	250	100	240	240	240	(0,0,0)	(250,0,0)	(250,200,0)	A(-100, -100, 100) B(-100, 350, 100) C(200, 350, 100) D(200, -100, 100) E(67.5, 120, 100) F(0, 120, 100) G(100, 200, 100) H(100, 50, 100)

The analysis was performed for each variable receiver coil position (A→H). The self-inductances and mutual inductances of the donor coils are presented in Table 2 and the magnetic flux change in the case of center alignments of the transmitter coils and the receiver coil is shown in Figure 3. It is seen in the table that the self-inductance values of the transmitter coils and the receiver coil are constant.

Table 2. Self-inductance and mutual inductance values for A→H positions of the receiver coil (Alıcı bobinin A→H konumları için öz endüktans ve karşılıklı endüktans değerleri)

		Receiver Coil Positions							
		A	***B***	***C***	***D***	***E***	***F***	***G***	***H***
Self-Inductances(μH)	***TX_1***	*57.315*	*57.165*	*57.028*	*57.165*	*57.031*	*57.029*	*57.031*	*57.026*
	TX_2	*57.187*	*57.026*	*57.170*	*57.026*	*57.035*	*57.029*	*57.029*	*57.035*
	TX_3	*56.442*	*56.429*	*56.430*	*56.429*	*56.427*	*56.427*	*56.428*	*56.427*
	RX	*57.035*	*57.167*	*56.176*	*57.167*	*57.008*	*57.069*	*57.008*	*57.021*
Mutual Inductances(μH)	***M_{12}***	*-2.419*	*-2.475*	*-2.475*	*-2.475*	*-2.482*	*-2.482*	*-2.482*	*-2.482*
	M_{13}	*-2.656*	*-2.664*	*-2.682*	*-2.664*	*-2.683*	*-2.683*	*-2.683*	*-2.683*
	M_{23}	*-2.748*	*-2.757*	*-2.739*	*-2.757*	*-2.758*	*-2.758*	*-2.758*	*-2.758*
	M_{1R}	*0.514*	*-1.868*	*-0.204*	*-1.918*	*-0.786*	*5.612*	*-2.058*	*3.919*
	M_{2R}	*-0.377*	*0.446*	*-1.797*	*-0.231*	*0.528*	*0.682*	*0.111*	*-1.977*
	M_{3R}	*-0.290*	*-0.668*	*-1.957*	*-2.122*	*-0.445*	*-2.168*	*-1.409*	*2.516*

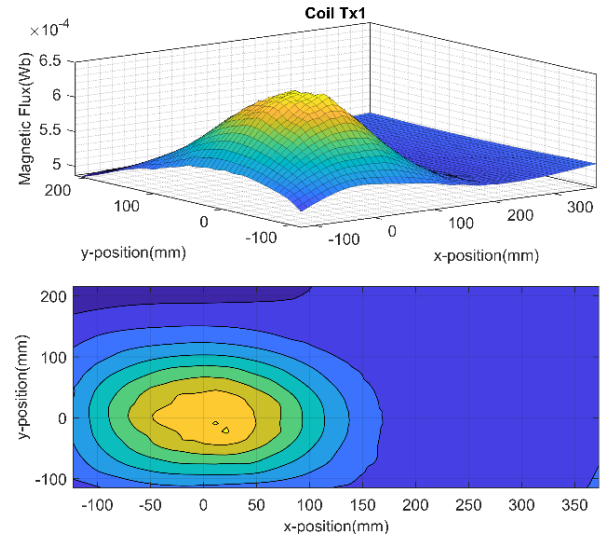

(a)

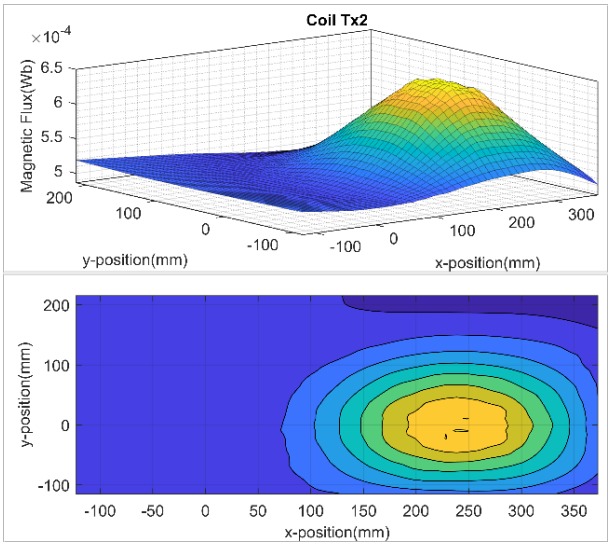

(b)

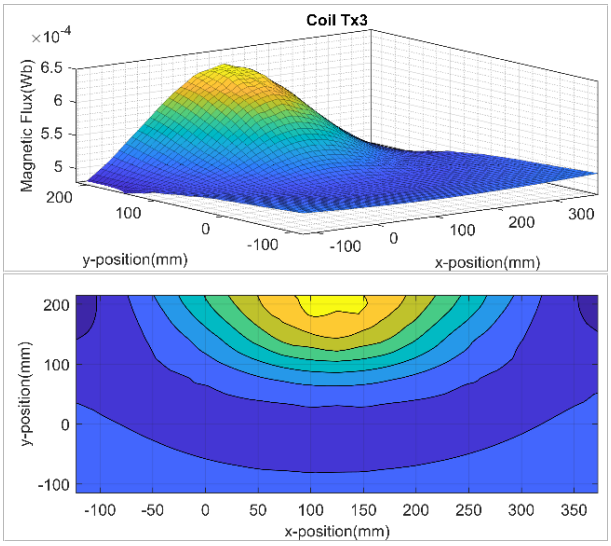

(c)

Figure 3. Magnetic flux change with the centers of the transmitter coils and the receiving coil aligned (Merkezleri hizalanmış, verici bobin ve alıcı bobine ait manyetik akı değişimi)

It is evident that the mutual inductances of the transmitter coils, M_{12}, M_{23}, and M_{13}, vary based on the position changes of the receiving coil. Again, it can be seen that the mutual inductance value of M_{1R}, M_{2R}, and M_{3R} between each transmitter coil and the receiving coil varies drastically. These mutual inductance values directly change the efficiency η value given in Equation 11 and affect the system's efficiency. It is possible to reduce this effect by changing the C_T capacity in the transmitting circuit.

The control of C_T capacity was done with the help of the algorithm presented in a previous study, and the efficiency analysis of the system was made in Section 4 [22]. The flow diagram of the algorithm used is given in Figure 4.

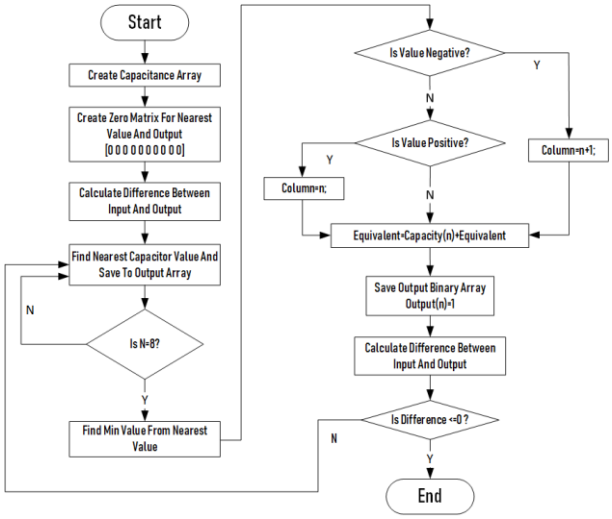

Figure 4. Capacity calculation algorithm(Kapasite hesaplama algoritması)[22]

Equivalent impedance calculations for the cases where the capacity array is applied and not applied are calculated as given in Figure 5. In the computation, equivalent impedance values were obtained for the resonant frequency of the system 85Khz. The impedance change for each coil position (A to H) was analyzed.

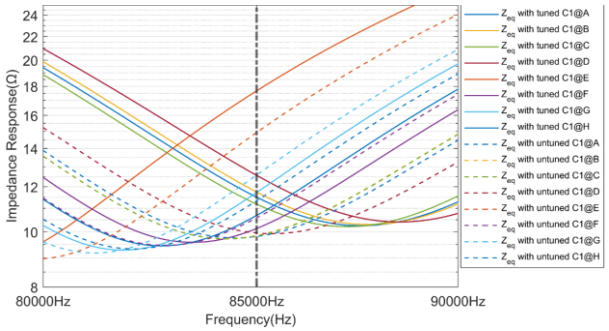

Figure 5. Equivalent impedance of WPT system with/without tuned capacitor array for positions A to H (A'dan H'ye kadar olan konumlar için adaptif kapasite

dizisi uygulanan/uygulanmayan WPT sisteminin eşdeğer empedansı)

By calculating the efficiency of the system according to the impedance change, the graph was obtained in Figure 6. In the chart, it is seen that the efficiency for points A, B, C, D, and E increased by 1.78%, 1.97%, 1.48%, 2.52%, and 1.30%, respectively. Adjusting the capacity array for positions F, G, and H resulted in a decrease in efficiency. The capacity array was underestimated because the mutual inductance was negative if the receiver coil was positioned at the midpoints of the transmitter coils with each other. For this reason, a decrease in efficiency has occurred at these points. Here, it is concluded that the algorithm used in capacitance array tuning cannot respond to the negative variation of mutual inductance.

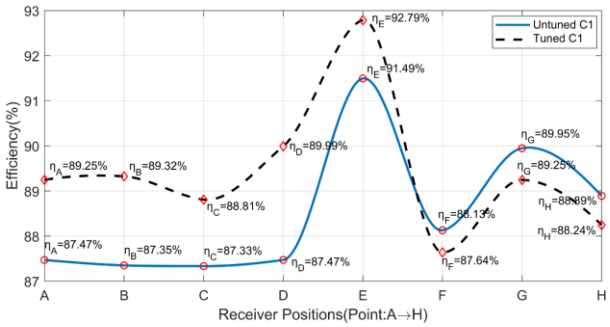

Figure 6. Efficiency analysis of tuned/untuned capacitor from A to H (A'dan H'ye ayarlanmış /ayarlanmamış kapasitenin verimlilik analizi)

4. EXPERIMENTAL RESULTS (DENEYSEL SONUÇLAR)

The experimental study consists of five main parts, as given in Figure 7. The main parts are the power and control card (A), the transmitter coil group (B), the receiver coil (C), the receiving circuit power card (D) and the digital signal processor (DSP) that provides the control of the system. The grid voltage is rectified using the uncontrolled rectifier circuit (F) in the power and control card, and the high-frequency inverter DC bus voltage is produced. The DC Bus voltage is applied to the Mosfets (K) to create a high-frequency full bridge inverter with 85 kHz switching frequency. The drive circuits (I and J) are fed using the drive supply circuits (G and H) of the Mosfets. The switching signals of the drives are generated by the DSP and controlled operation of the inverter is ensured. High-frequency voltage is applied to the transmitter coil group (B) over the parallel capacity (L) at the inverter output. The measurement of the output current and voltage required to control the inverter is carried out by the measuring circuit (M). The obtained measurement signals are converted by amplification, filtering, and Zero-crossing detector circuit(N) to a level the DSP can detect. Here, the Zero-Crossing detector circuit calculates the phase difference between current and voltage.

The energy transferred by the transmitter coil group is transferred by the receiver coil (C) to the receiving circuit power board (D). The energy is transferred to the receiver load (P) via the resonant capacitor (O) placed by the system's resonant frequency on the receiving circuit power board. Experimental studies were carried out using this mechanism.

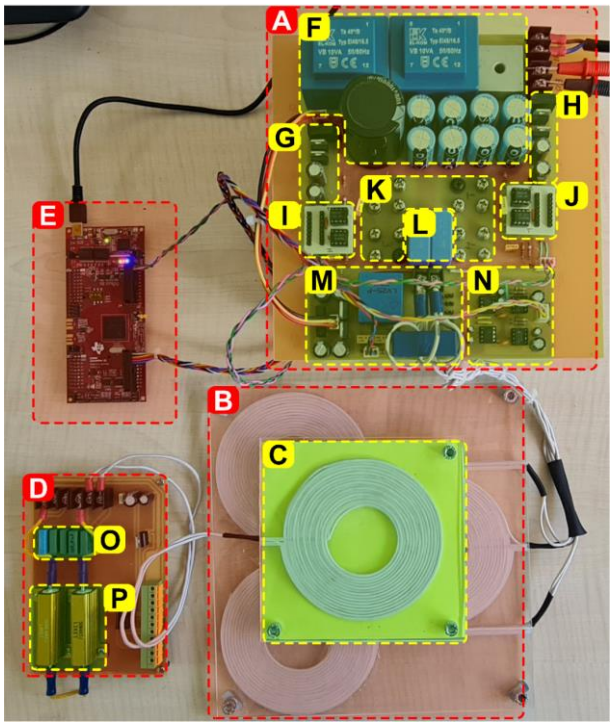

Figure 7. Main parts of the experimental set (Deney setinin ana bileşenleri)

In the first experimental study, the receiver coil was positioned in position A, and current, voltage, and phase difference measurements were performed. The results presented in Figure 8 were obtained.

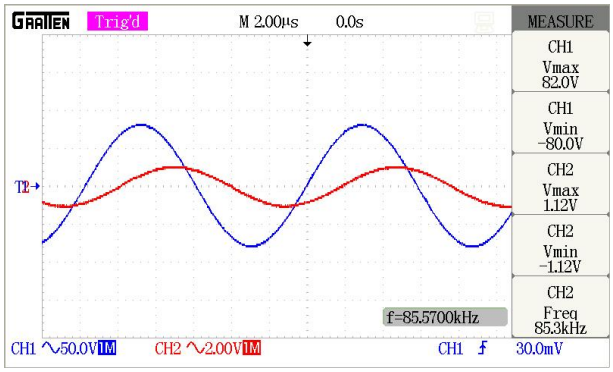

Figure 8. Voltage-current graph for positions A and B (A ve B konumları için gerilim-akım grafiği)

In this experiment, the transmitted power was realized as 660.23W, and the phase difference was

measured as 43.94º. The same experiment was performed in position B; the transmitted power was 659.34W, and the phase difference was 44.21º.

The test was repeated by bringing the receiver coil to the C position. The power obtained at this position was 556.48W, and the phase difference was 41.99º. When the receiver coil is turned to the D position, 553.32W power, and 42.08º phase difference are obtained. The same results were obtained at both locations, and the voltage-current graphs are presented in Figure 9.

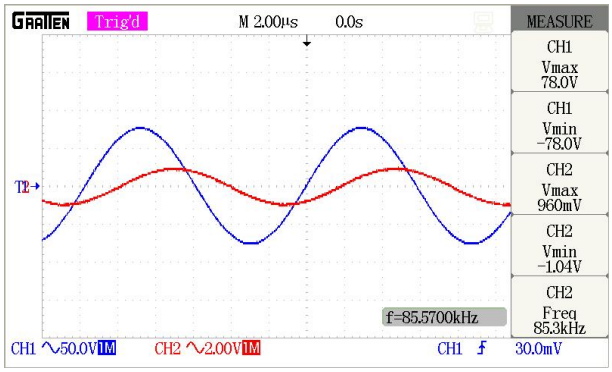

Figure 9. Voltage-current graph for positions C and D (C ve D konumları için gerilim-akım grafiği)

The receiver coil position has been moved to the E position at the center point of the transmitter coils. At this position, 864.90W of power was transmitted with a phase difference of 39.44º. The voltage and current graph of the experiment are given in Figure 10.

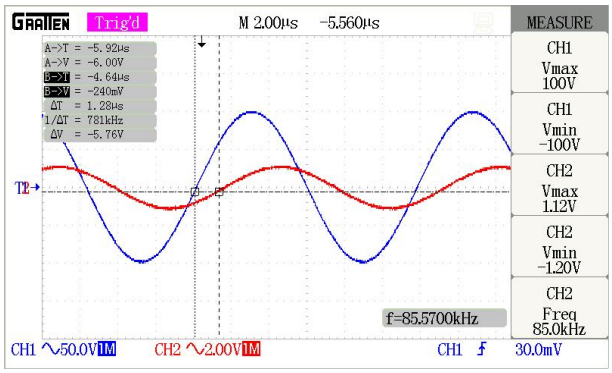

Figure 10. Voltage-current graph for position E (E konumu için gerilim-akım grafiği)

Here, unlike previous experiments (A-D positions), it was observed that the transferred power increased and the phase difference decreased. The better alignment of the transmitter coil group and the receiving coil increased the flowing energy, and the phase difference decreased due to the approximately equal mutual inductance between the coils.

When the receiver coil is moved to the F position, the transmitted power is obtained as 961.87W, and the phase difference is 30.81º. The obtained voltage-current graphs are given in Figure 11. Here, the transferred power increased and the phase difference decreased because of the mutual inductance both of the transmitter coils was positive and the mutual inductance between the other coil was negative.

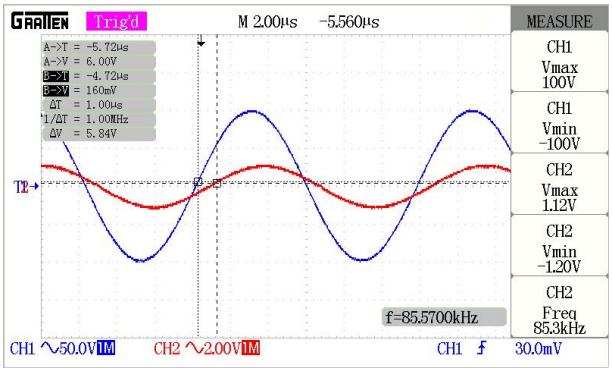

Figure 11. Voltage-current graph for position F (F konumu için gerilim-akım grafiği)

When the coil position is brought to the G-point, the transmitted power is 594.60W, and the phase difference is 57.93º. The voltage-current graphs of the experiment are presented in Figure 12.

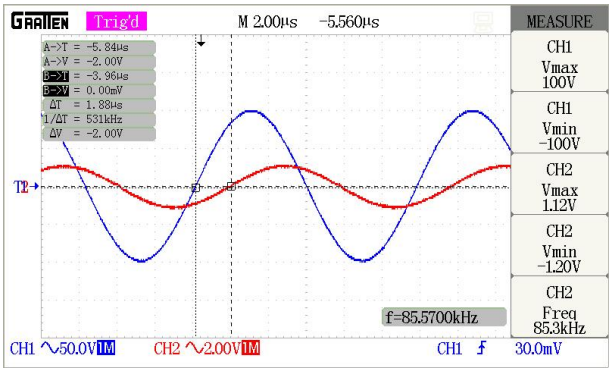

Figure 12. Voltage-current graph for position G (G konumu için gerilim-akım grafiği)

In the experiment, the mutual inductance between two of the transmitter coils was negative, and the mutual inductance with the other coil was positive, which disrupted the inverter load match, so the transferred power decreased.

In the last experiment, the power transferred in the receiving coil brought to the H position was 553.22W, and the phase difference was obtained as 60.93º. Because the receiver coil position is similar to the situation in position G, the transferred power and phase difference values remained approximately equal. The obtained voltage-current graphs are presented in Figure 13.

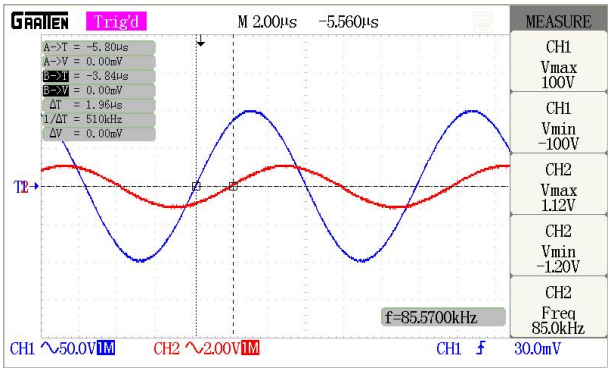

Figure 13. Voltage-current graph for position H (H konumu için gerilim-akım grafiği)

In the experiments carried out so far, the transmitter circuit capacity has not been tuned and has been kept constant. In the experiments at constant capacity value, the highest power transferred according to the receiver coil position was 961.87W, and the lowest was 553.22W. The experimental study was tested by repositioning the receiver coil to the E position, which is the center point of the transmitter coils, and applying the tuned capacity. The adjusted capacity application was carried out with the capacity calculation application, the flow diagram of which is presented in Figure 4, and results are presented in Figure 14.

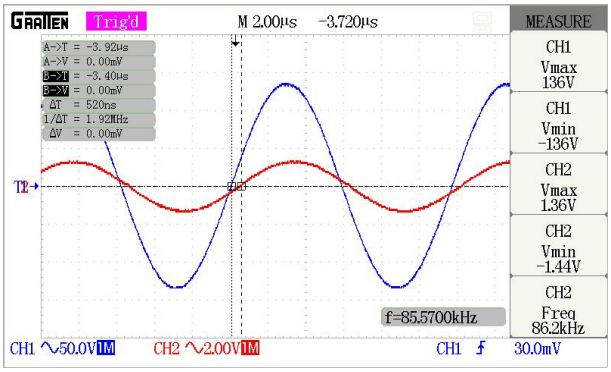

Figure 14. Voltage-current graph using tuned capacitor for position E (E konumu için adaptif kapasite dizisi uygulandığında gerilim-akım grafiği)

As a result of the application, the power value transferred at point E increased from 864.90W to 1307.15W. In addition, the phase difference obtained in the application without capacity adjustment was reduced from 39.44° to 16.02°. It has been achieved to increase the value of transmitted power by approximately 33%. All experiments were repeated for A to H positions, data were obtained, and the efficiency calculation of the system was made according to Equation 12. The measured efficiency and the efficiency values obtained in the simulation study are compared in Figure 15.

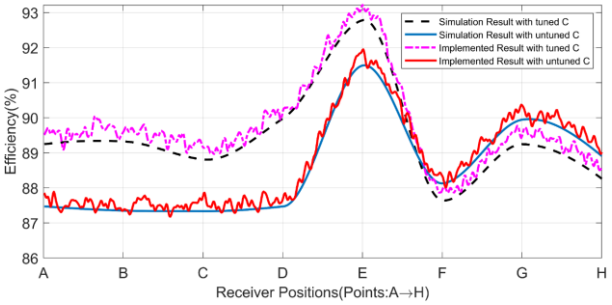

Figure 15. Efficiency analysis with/without tuned capacitor from A to H (A'dan H'ye adaptif kapasite dizisi uygulanmış/uygulanmamış durumlar için verimlilik analizi)

In the simulation results without capacity tuning, the efficiency varied between the lowest, 84.95%, and the highest, 91.49%. In experiments conducted without capacity tuning for the exact locations, the efficiency was calculated as the lowest at 87.36% and the highest at 91.93%. In the simulation results where capacity tuning was made, the efficiency varied between the lowest, 88.13%, and the highest, 92.79%. In the experiments where capacity tuning was made for the same positions, the efficiency was calculated as the lowest at 89.51% and the highest at 93.11%. Approximately the same rates of change were obtained. The calculated and obtained efficiency values overlap when all the simulation and experimental study results are evaluated.

5. CONCLUSIONS (SONUÇLAR)

A wireless energy transfer system with multiple transmitting coils uses a full bridge inverter with an operating frequency of 85Khz. Three transmitters and one receiver coil used in the system were modeled and applied. The situations in which the tuned capacity array is used and not used in the system are discussed, and its effect on the system's efficiency is investigated. Simulation and application studies were carried out for eight different receiver coil placements. In the simulation studies, efficiency analysis was performed for the situations where there was and no capacity tuning. In the simulation results, the efficiency was obtained between the lowest, 87.5%, and the highest, 91.5%. Under the same conditions, efficiency analysis was performed in the experimental study. The lowest was 87.8%, and the highest was 91.9%. Simulation and experimental studies were repeated with the tuned capacity array. In the simulation study, the efficiency was between the lowest 89.3% and the highest 92.8%, and in the experimental study, the lowest 89.5% and the highest 93.1%. As a result of the experimental study, it was seen that the efficiency was increased by 1.65%, 1.23%, 1.39%, 2.5%, and 1.28% for five different locations (A→E), respectively, while it

decreased by 0.4%, 0.89% and 0.45% for three other locations (F→H), respectively. In cases of reduced efficiency, it was concluded that the resolution of the capacities in the tuned capacity application was not sensitive enough. In future studies, it is necessary to conduct comprehensive studies such as capacity tuning with higher resolution and using different control algorithms.

ACKNOWLEDGMENTS (TEŞEKKÜR)

This study was supported by the Cankiri Karatekin University Research Projects Unit with the code 2023/MYO240223B08.

Bu çalışma Çankırı Karatekin Üniversitesi Bilimsel Araştırma Projeleri Birimi tarafından 2023/MYO240223B08 kodu ile desteklenmiştir.

DECLARATION OF ETHICAL STANDARDS (ETİK STANDARTLARIN BEYANI)

The author of this article declares that the materials and methods they use in their work do not require ethical committee approval and/or legal-specific permission.

Bu makalenin yazarı çalışmalarında kullandıkları materyal ve yöntemlerin etik kurul izni ve/veya yasal-özel bir izin gerektirmediğini beyan ederler.

AUTHORS' CONTRIBUTIONS (YAZARLARIN KATKILARI)

***Fatih ISSI*:** He conducted the experiments, analyzed the results and performed the writing process.

Deneyleri yapmış, sonuçlarını analiz etmiş ve maklenin yazım işlemini gerçekleştirmiştir.

CONFLICT OF INTEREST (ÇIKAR ÇATIŞMASI)

There is no conflict of interest in this study.

Bu çalışmada herhangi bir çıkar çatışması yoktur.

REFERENCES (KAYNAKLAR)

[1] H. L. Li, A. P. Hu, G. A. Covic, and C. S. Tang, "Optimal coupling condition of IPT system for achieving maximum power transfer," (in English), Electron Lett, vol. 45, no. 1, pp. 76-U25, Jan 1 2009, doi: 10.1049/el:20091886.

[2] A. Mahesh, B. Chokkalingam, and L. Mihet-Popa, "Inductive Wireless Power Transfer Charging for Electric Vehicles–A Review," Ieee Access, vol. 9, pp. 137667-137713, 2021, doi: 10.1109/ACCESS.2021.3116678.

[3] G. R. Nagendra, G. A. Covic, and J. T. Boys, "Sizing of Inductive Power Pads for Dynamic Charging of EVs on IPT Highways," IEEE Transactions on Transportation Electrification, vol. 3, no. 2, pp. 405-417, 2017, doi: 10.1109/TTE.2017.2666554.

[4] S. Kim, A. Zaheer, G. Covic, and J. Boys, "Tripolar pad for inductive power transfer systems," in IECON 2014 - 40th Annual Conference of the IEEE Industrial Electronics Society, 29 Oct.-1 Nov. 2014 2014, pp. 3066-3072, doi: 10.1109/IECON.2014.7048947.

[5] J. Deng, W. Li, T. D. Nguyen, S. Li, and C. C. Mi, "Compact and Efficient Bipolar Coupler for Wireless Power Chargers: Design and Analysis," IEEE Transactions on Power Electronics, vol. 30, no. 11, pp. 6130-6140, 2015, doi: 10.1109/TPEL.2015.2417115.

[6] A. Bharadwaj, A. Sharma, and C. R. Chandupatla, "A Switched Modular Multi-Coil Array Transmitter Pad With Coil Rectenna Sensors to Improve Lateral Misalignment Tolerance in Wireless Power Charging of Drone Systems," IEEE Transactions on Intelligent Transportation Systems, vol. 24, no. 2, pp. 2010-2023, 2023, doi: 10.1109/TITS.2022.3220793.

[7] A. P. Sample, D. A. Meyer, and J. R. Smith, "Analysis, Experimental Results, and Range Adaptation of Magnetically Coupled Resonators for Wireless Power Transfer," (in English), Ieee Transactions on Industrial Electronics, vol. 58, no. 2, pp. 544-554, Feb 2011, doi: 10.1109/Tie.2010.2046002.

[8] E. S. Lee, D. Kim, and S. Y. Jeong, "Triangular DQ Tx Coils of Wireless EV Chargers for Large Misalignment Tolerances," IEEE Transactions on Vehicular Technology, vol. 72, no. 11, pp. 14179-14188, 2023, doi: 10.1109/TVT.2023.3288553.

[9] V. K. Srivastava and A. Sharma, "Optimized 3-D Polarized-Field Forming for Orientation-Insensitive Wireless Power Transfer Systems," (in English), Ieee Transactions on Antennas and Propagation, vol. 69, no. 8, pp. 4999-5007, Aug 2021, doi: 10.1109/Tap.2021.3060140.

[10] K. Aditya, V. K. Sood, and S. S. Williamson, "Magnetic Characterization of Unsymmetrical Coil Pairs Using Archimedean Spirals for Wider Misalignment Tolerance in IPT Systems," (in English), Ieee Transactions on Transportation Electrification, vol. 3, no. 2, pp. 454-463, Jun 2017, doi: 10.1109/Tte.2017.2673847.

[11] C. C. Huang, C. L. Lin, J. J. Kao, J. J. Chang, and G. J. Sheu, "Vehicle Parking Guidance for Wireless Charge Using GMR

Sensors," IEEE Transactions on Vehicular Technology, vol. 67, no. 8, pp. 6882-6894, 2018, doi: 10.1109/TVT.2018.2827069.

[12] J. Liu, "Research and Implementation of Electric Vehicle Fast Charging Station Parking Guidance System Based on Mobile Terminal," in 2017 9th International Conference on Intelligent Human-Machine Systems and Cybernetics (IHMSC), 26-27 Aug. 2017 2017, vol. 1, pp. 230-233, doi: 10.1109/IHMSC.2017.60.

[13] T. S. Lee, S. J. Huang, S. H. Dai, and J. L. Su, "Design of Misalignment-Insensitive Inductive Power Transfer via Interoperable Coil Module and Dynamic Power Control," IEEE Transactions on Power Electronics, vol. 35, no. 9, pp. 9024-9033, 2020, doi: 10.1109/TPEL.2020.2972035.

[14] Y. Chen et al., "A Hybrid Inductive Power Transfer System With Misalignment Tolerance Using Quadruple-D Quadrature Pads," IEEE Transactions on Power Electronics, vol. 35, no. 6, pp. 6039-6049, 2020, doi: 10.1109/TPEL.2019.2954906.

[15] B. Yang, Y. Chen, W. Ruan, H. Liu, Y. Ren, and R. Mai, "Current Stress Optimization for Double-Sided CLLLC Topology-Based IPT System With Constant Output Current Tolerating Pad Misalignments," IEEE Transactions on Industry Applications, vol. 58, no. 1, pp. 1032-1043, 2022, doi: 10.1109/TIA.2021.3125281.

[16] J. L. Villa, J. Sallan, J. F. S. Osorio, and A. Llombart, "High-Misalignment Tolerant Compensation Topology For ICPT Systems," IEEE Transactions on Industrial Electronics, vol. 59, no. 2, pp. 945-951, 2012, doi: 10.1109/TIE.2011.2161055.

[17] J. Kim, D. H. Kim, and Y. J. Park, "Analysis of Capacitive Impedance Matching Networks for Simultaneous Wireless Power Transfer to Multiple Devices," IEEE Transactions on Industrial Electronics, vol. 62, no. 5, pp. 2807-2813, 2015, doi: 10.1109/TIE.2014.2365751.

[18] J. M. Miller, O. C. Onar, and M. Chinthavali, "Primary-Side Power Flow Control of Wireless Power Transfer for Electric Vehicle Charging," (in English), Ieee Journal of Emerging and Selected Topics in Power Electronics, vol. 3, no. 1, pp. 147-162, Mar 2015, doi: 10.1109/Jestpe.2014.2382569.

[19] E. S. Lee, "Frequency-Modulation-Based IPT With Magnetic Communication for EV Wireless Charging," IEEE Transactions on Industrial Electronics, vol. 70, no. 2, pp. 1398-1408, 2023, doi: 10.1109/TIE.2022.3158027.

[20] E. S. Lee, B. G. Choi, J. S. Choi, D. T. Nguyen, and C. T. Rim, "Wide-Range Adaptive IPT Using Dipole-Coils With a Reflector by Variable Switched Capacitance," (in English), Ieee Transactions on Power Electronics, vol. 32, no. 10, pp. 8054-8070, Oct 2017, doi: 10.1109/Tpel.2016.2637931.

[21] W. V. Wang, D. J. Thrimawithana, and M. Neuburger, "An Si MOSFET-Based High-Power Wireless EV Charger With a Wide ZVS Operating Range," (in English), Ieee Transactions on Power Electronics, vol. 36, no. 10, pp. 11163-11173, Oct 2021, doi: 10.1109/Tpel.2021.3071516.

[22] F. Issi and O. Kaplan, "Manyetik Rezonans Kuplajlı Kablosuz Enerji Transfer Sistemi için Empedans Analizi ve Değişken Kapasite Dizisi Uygulaması," Gazi University Journal of Science Part C: Design and Technology, vol. 8, no. 4, pp. 1005-1020, December 2020, doi: 10.29109/gujsc.817922.